

Complexes of urea with Mn(II), Fe(III), Co(II), and Cu(II) metal ions

Omar B. Ibrahim

*Department of Chemistry, Faculty of Science, Taif University, Al-Hawiah, Taif, P.O. Box 888
Zip Code 21974, Saudi Arabia*

ABSTRACT

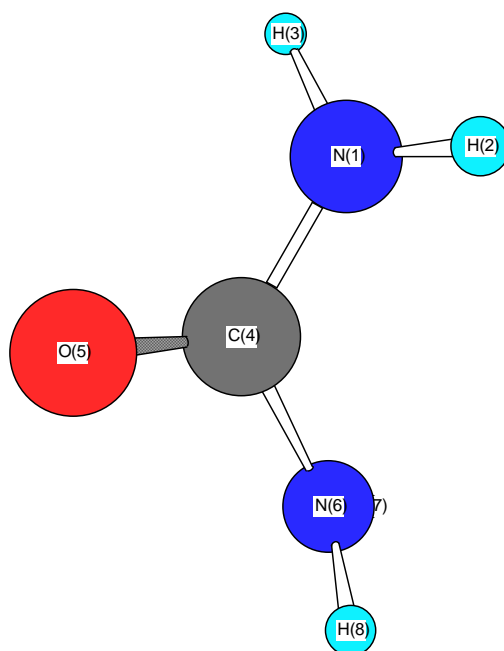
The complexation of urea (U) with manganese(II), cobalt(II), iron(III) and copper(II) ions at different temperatures has been studied by many methods namely elemental analysis, magnetic susceptibility, conductivity measurements, infrared and thermal analysis (TG/DTG), scanning electron microscopy (SEM), Energy-dispersive X-ray spectroscopy (EDX), and x-ray powder diffraction (XRD). The high values of molar conductivity of the resulting urea complexes show them to be electrolytes in nature. The physical and spectral data were well explained in terms of the formation of $\text{CuCl}_2 \cdot 2\text{U} \cdot 4\text{H}_2\text{O}$ (1), $\text{CuCl}_2 \cdot 2\text{U} \cdot 2\text{H}_2\text{O}$ (2), $\text{CO}(\text{NO}_3)_2 \cdot 6\text{U}$ (3), $\text{CO}(\text{NO}_3)_2 \cdot 2\text{U} \cdot 4\text{H}_2\text{O}$ (4), $\text{FeCl}_2 \cdot 6\text{U} \cdot 3\text{H}_2\text{O}$ (5), $\text{FeCl}_2 \cdot 3\text{U} \cdot 5\text{H}_2\text{O}$ (6), $\text{MnCl}_2 \cdot 3\text{U} \cdot 3\text{H}_2\text{O}$ (7), $\text{MnCl}_2 \cdot 6\text{U}$ (8). Complexes of urea (1, 3, 5 and 7), and (2, 4, 6 and 8) were synthesized at room temperature and 60°C , respectively. On the basis of the infrared spectral data and the values of stretching vibrational bands of both $-\text{C}=\text{O}$ and $-\text{NH}_2$ groups, the complexation of metal ions toward urea was distinguished. The enhancement of the microbial treatments against bacteria (*Escherichia Coli*, *Staphylococcus Aureus*, *Bacillus subtilis* and *Pseudomonas aeruginosa*) and fungi (*Aspergillus Flavus* and *Candida Albicans*) was assessed and a remarkable efficiency was recorded.

Keywords: Urea, Transition metals, Biological activity, Conductance, Spectroscopic studies, Thermal analysis.

INTRODUCTION

Carbamide, carbonyldiamide or the most famous name, urea (Scheme 1), $\text{CH}_4\text{N}_2\text{O}$, was first prepared by Wöhler [1] by evaporating a solution containing a mixture of potassium isocyanate and ammonium sulphate. Ammonium isocyanate, which is formed first, undergoes molecular rearrangement to give urea, as shown by the following reaction;



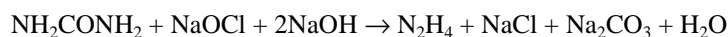


Scheme 1: Structure of urea

Urea may be prepared in the laboratory by the action of ammonia with carbonyl chloride, alkyl carbonates, chloroformates or urethans. Industrially [2-4], urea is prepared by allowing liquid carbon dioxide and liquid ammonia to interact, and heating the formed ammonium carbamate at 130-150 °C under about 35 atmospheric pressure. The carbamate is decomposed to form urea and water according to the following reaction;



Urea is physiologically very important. It is the chief nitrogenous product of protein metabolism. Adults excrete about 30g of urea per day in the urine, from which it can be extracted by evaporating the urine to small volume and adding nitric acid, to give the slightly soluble urea nitrate, $\text{CO}(\text{NH}_2)_2 \cdot \text{HNO}_3$. Urea has a melting point of 132°C, soluble in water and ethanol, but insoluble in ether. Urea is used for preparing formaldehyde-Urea resin (plastics) [5], barbiturates [6], and fertilizers [7-10]. Urea is also extensively used in the paper industry to soften cellulose and has been used to promote healing in infected wounds and many other applications in the field of medicine [11-13]. Recently, urea is used for the manufacture of hydrazine in which urea is treated with alkaline sodium hypochlorite [6] e.g.,



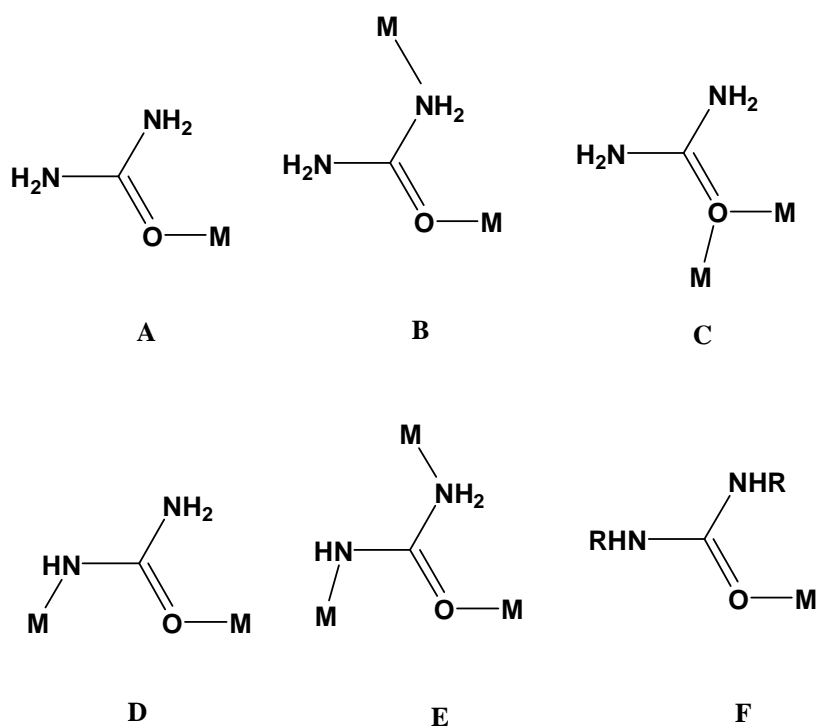
Urea is used in reactive dyeing [14] which has an effect on the formation and cleavage of covalent bond between the reactive dye and cellulose. The overall effect of urea on reactive dyeing depends on the solvolytic stability of the dye-fiber bond under specific dyeing conditions.

Complexes of urea with some metal ions are used as fertilizers [15-18]. Complexes of urea with zinc sulphate and nitrate, $[\text{Zn}(\text{CON}_2\text{H}_4)_6]\text{SO}_4 \cdot \text{H}_2\text{O}$ and $[\text{Zn}(\text{CON}_2\text{H}_4)_4](\text{NO}_3)_2 \cdot 2\text{H}_2\text{O}$ have very important application in this field [19]. These complexes were found to increase the yield of rice more than a dry mixture of urea-zinc salt does. Calcium nitrate-urea complex, $[\text{Ca}(\text{urea})_4](\text{NO}_3)_2$, [20,21] was used also as an adduct fertilizer. Some metal-urea complexes have pharmaceutical application, e.g., the platinum-urea complex which is used as antitumor [22].

Crystal structure studies have shown that in solid urea, both nitrogen atoms are identical. Bond length measurements [6] in urea give the C-N distance as 1.37\AA , while, in aliphatic amines the C-N bond length is 1.47\AA . This indicates that the C-N bond in urea has some double bond character (about 28%).

Urea usually coordinates as a monodentate ligand through the oxygen atom, forming a $\text{C}=\text{O} \cdots \text{M}$ angle considerably smaller than 180° , in accordance with the sp^2 hybridization of the O atom (**A** in Scheme 2). The rare N,O-bidentate coordination mode (**B** in Scheme 2) has been found in a very limited number of cases [23, 24], while in $[\text{Hg}_2\text{Cl}_4\text{U}_2]$ each U molecule bridges the two Hg^{II} atoms through the oxygen atom [25] (**C** in Scheme 2). Of particular

chemical/biological interest is the ability of U to undergo metal-promoted deprotonation [26]; the monoanionic ligand H_2NCONH^- adopts the $\mu 2$ (**D** in Scheme 2) and $\mu 3$ (**E** in Scheme 2) coordination modes. The urea and its derivatives such as the $\text{N,N}'$ -dimethylurea and $\text{N,N}'$ -diethylurea (Scheme 2) have only been found to coordinate as monodentate ligands through the oxygen atom (**F** in Scheme 2).



Scheme 2: The coordination modes of urea towards metal ions

Raman and infrared spectra of urea have been observed by several investigators [27-32]. The normal vibrations of the urea molecule were calculated by Kellner [33] on the assumption of the non-planar model. However, on the basis of the dichronic measurement of the infrared band arising from the N-H stretching vibration by Waldron and Badger [34] and the proton magnetic resonance absorption measurement made by Andrew and Hyndman [35], it is concluded that urea molecule has a planar structure. Yamaguchi et al. [36] calculated the normal vibrations of the C_{2v} model of urea molecule as an eight-body problem using a potential function of the Urey-Bradley force field and obtained the force constants which have been refined by the least-squares method. Based on the result of these calculations, Yamaguchi [36], assigned all of the observed frequencies in the spectra of urea and urea- d_4 . To the two vibrations of the frequencies 1686 and 1603cm^{-1} , there are considerable contributions of both CO stretching and NH_2 bending motions, whereas Stewart [37] assigned the 1686cm^{-1} band to CO stretching vibration and the 1603cm^{-1} band to NH_2 bending motion. The calculations studied by Yamaguchi showed that for the band at 1686cm^{-1} , the contribution of the NH_2 bending motion is greater than that of CO stretching motion. The band at 1629cm^{-1} corresponds to almost pure NH_2 bending vibration. The NH_2 bending motion of A_1 type is equal to that of B_2 type. The A_1 type band should have a frequency of about 1630cm^{-1} , if there is no coupling between NH_2 bending and CO stretching motions. On the other hand, the observed frequency of 1610cm^{-1} of urea- d_4 is assigned to almost pure skeletal vibration. Therefore, the interaction between the 1630 and 1610cm^{-1} vibration gives rise to the two observed bands at 1686 and 1603cm^{-1} . The infrared bands of urea- d_4 observed at 1245 and 1154cm^{-1} are assigned, respectively, to A_1 type and B_2 type, ND_2 bending vibrations. This assignment is consistent with the observed depolarization degrees of the Raman lines. The large frequency difference between the A_1 and B_2 vibrations is due to the fact that in the A_1 vibration, the cross term related to the CN stretching vibration is large.

The 1464cm^{-1} frequency of urea is assigned to the CN stretching vibration of B_2 type. The corresponding frequency of urea- d_4 is observed at 1490cm^{-1} . The 1150cm^{-1} band is assigned to NH_2 rocking vibrations of both A_1 and B_2 types. The normal vibration calculation yields almost the same values for these frequencies.

Urea possesses two types of potential donor atoms, the carbonyl oxygen and amide nitrogens. Penland et al. [38] studied the infrared spectra of urea complexes to determine whether coordination occurs through oxygen or nitrogen atoms. The electronic structure of urea may be represented by a resonance hybrid of structures **A-F** as shown in scheme 1 with each contributing roughly an equal amount. If coordination occurs through nitrogen, contributions of

structure **B** will decrease. This results in an increase of the CO stretching frequency with a decrease of CN stretching frequency. The N-H stretching frequency in this case may fall in the same range as those of the amido complexes. If coordination occurs through oxygen, the contribution of structure (**A**) will decrease. This may result in a decrease of the CO stretching frequency but no appreciable change in NH stretching frequency. Since the vibrational spectrum of urea itself has been analyzed completely [36], band shifts caused by coordination can be checked immediately. For example, the effect of the coordination on the spectra of the complexes of urea with Pt(II) and Cr(III) in which the coordination occurs through nitrogen and oxygen atoms, respectively [38]. The mode of coordination of urea with metal ions seems to be dependent upon the type and nature of metal. Pd(II) coordinates to the nitrogen, whereas Fe(III), Zn(II), and Cu(II) coordinate to the oxygen of urea [38].

In urea-metal complexes, if a nitrogen-to-metal bond is present, the vibrational spectrum of this complex differs significantly from that of the free urea molecule. The N-H stretching frequencies would be shifted to lower values, and the C=O bond stretching vibration, ($\nu(\text{C}=\text{O})$) would be shifted to higher frequency at about 1700cm^{-1} [39].

Recently, urea represents not only an important molecule in biology [40] but also an important raw material in chemical industry [41]. The aim of this publication is to report the synthesis, characterization, conductance and biological studies of the resulting compounds formed from the reactions of urea with AgNO_3 , $\text{CrCl}_3 \cdot 6\text{H}_2\text{O}$, $\text{CdCl}_2 \cdot \text{H}_2\text{O}$ and ZnCl_2 at room, elevated and ignition temperatures.

MATERIALS AND METHODS

2-1- Materials

Urea, $\text{CuCl}_2 \cdot 2\text{H}_2\text{O}$, $\text{Co}(\text{NO}_3)_2 \cdot 6\text{H}_2\text{O}$, $\text{FeCl}_3 \cdot 6\text{H}_2\text{O}$, MnCl_2 and methanol solvent were obtained from Aldrich Company. Urea was received from Fluka chemical company. All chemicals used in this study were of analytical grade and they were used without further purification.

2-2- Synthesis of Cu(II), Co(II), Fe(II) and Mn(II) urea complexes

2-2-1- Synthesis of urea complexes at room temperature

The complexes, $\text{CuCl}_2 \cdot 2\text{U} \cdot 4\text{H}_2\text{O}$ (**1**), $\text{Co}(\text{NO}_3)_2 \cdot 6\text{U}$ (**3**), $\text{FeCl}_2 \cdot 6\text{U} \cdot 3\text{H}_2\text{O}$ (**5**) and $\text{MnCl}_2 \cdot 3\text{U} \cdot 3\text{H}_2\text{O}$ (**7**) were prepared by mixing equal methanolic solutions of $\text{CuCl}_2 \cdot 2\text{H}_2\text{O}$ (1.70 g, 0.01 mole), $\text{Co}(\text{NO}_3)_2 \cdot 6\text{H}_2\text{O}$ (2.91 g, 0.01 mole), $\text{FeCl}_3 \cdot 6\text{H}_2\text{O}$ (2.70 g, 0.01 mole) or MnCl_2 (1.98 g, 0.01 mole) in 25 mL methanol with a 50 mL volume of urea solution (2.40 g, 0.04 mole) in methanol solvent. The mixtures were stirred for about 12 hours under refluxed system at room temperature *Ca.* 25 °C. In all cases, the amount of the formed precipitate was increased with increasing the time of standing. The colored precipitated complex formed in each case was filtered off, dried under *vacuo* over anhydrous calcium chloride.

2-2-2- Synthesis of urea complexes at 60 °C temperature

The urea complexes, $\text{CuCl}_2 \cdot 2\text{U} \cdot 2\text{H}_2\text{O}$ (**2**), $\text{Co}(\text{NO}_3)_2 \cdot 2\text{U} \cdot 4\text{H}_2\text{O}$ (**4**), $\text{FeCl}_2 \cdot 3\text{U} \cdot 5\text{H}_2\text{O}$ (**6**) and $\text{MnCl}_2 \cdot 6\text{U}$ (**8**), were prepared by a method similar to that described for the preparation of urea complexes at room temperature. A 25 mL volume of urea solution (2.4g, 0.04 mole) was mixed with an equal volume of $\text{CuCl}_2 \cdot 2\text{H}_2\text{O}$ (1.70 g, 0.01 mole), $\text{Co}(\text{NO}_3)_2 \cdot 6\text{H}_2\text{O}$ (2.91 g, 0.01 mole), $\text{FeCl}_3 \cdot 6\text{H}_2\text{O}$ (2.70 g, 0.01 mole) or MnCl_2 (1.98 g, 0.01 mole) 25 mL methanol. The mixtures were stirred for about 2 hours then heated to 60 °C for 6 hours on a water bath under refluxed system. The precipitated products were filtered, dried at 60 °C in an oven for 3 hours.

2-3- Measurements

The elemental analyses of carbon, hydrogen and nitrogen contents were performed by the microanalysis unit at Cairo University, Egypt, using a Perkin Elmer CHN 2400 (USA). The molar conductivities of freshly prepared 1.0×10^{-3} mol/cm³ dimethylsulfoxide (DMSO) solutions were measured for the soluble urea complexes using Jenway 4010 conductivity meter. Magnetic measurements were performed on the Magnetic Susceptibility Balance, Sherwood Scientific, and Cambridge Science Park- Cambridge-England. The infrared spectra with KBr discs were recorded on a Bruker FT-IR Spectrophotometer ($4000\text{--}400\text{ cm}^{-1}$). The thermal studies TG/DTG-50H were carried out on a Shimadzu thermogravimetric analyzer under static air till 800 °C. Scanning electron microscopy (SEM) images and Energy Dispersive X-ray Detection (EDX) were taken in Joel JSM-6390 equipment, with an accelerating voltage of 20 KV. The X-ray diffraction patterns for the urea complexes were recorded on X'Pert PRO PANalytical X-ray powder diffraction, target copper with secondary monochromate.

2-4- Antibacterial and antifungal activities

Antimicrobial activity of the tested samples was determined using a modified Kirby-Bauer disc diffusion method [42]. Briefly, 100 μL of the best bacteria/fungi were grown in 10 mL of fresh media until they reached a count of approximately 10⁸ cells/mL for bacteria and 10⁵ cells/mL for fungi [43]. 100 μL of microbial suspension was spread

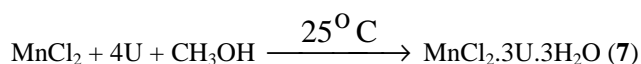
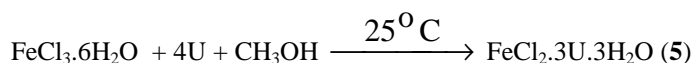
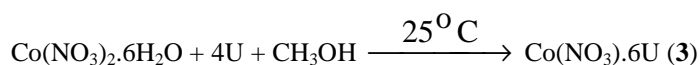
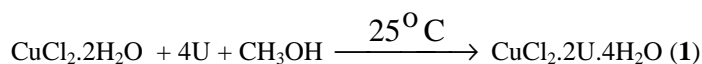
onto agar plates corresponding to the broth in which they were maintained. Isolated colonies of each organism that might be playing a pathogenic role should be selected from primary agar plates and tested for susceptibility by disc diffusion method [44, 45].

Of the many media available, National Committee for Clinical Laboratory Standards (NCCLS) recommends Mueller-Hinton agar due to: it results in good batch-to-batch reproducibility. Disc diffusion method for filamentous fungi tested by using approved standard method (M38-A) developed by the NCCLS [46] for evaluating the susceptibility of filamentous fungi to antifungal agents. Disc diffusion method for yeast developed standard method (M44-P) by the NCCLS [47]. Plates inoculated with filamentous fungi as *Aspergillus Flavus* at 25 °C for 48 hours; Gram (+) bacteria as *Staphylococcus Aureus*, *Bacillus subtilis*; Gram (-) bacteria as *Escherichia Coli*, *Pseudomonas aeruginosa* they were incubated at 35-37 °C for 24-48 hours and yeast as *Candida Albicans* incubated at 30 °C for 24-48 hours and, then the diameters of the inhabitation zones were measured in millimeters [42]. Standard discs of Tetracycline (Antibacterial agent), Amphotericin B (Antifungal agent) served as positive controls for antimicrobial activity but filter disc impregnated with 10 µl of solvent (distilled water, chloroform, DMSO) were used as a negative control.

The agar used is Mueller-Hinton agar that is rigorously tested for composition and pH. Further the depth of the agar in the plate is a factor to be considered in the disc diffusion method. This method is well documented and standard zones of inhabitation have been determined for susceptible values. Blank paper disks (Schleicher & Schuell, Spain) with a diameter of 8.0 mm were impregnated 10 µl of tested concentration of the stock solutions. When a filter paper disc impregnated with a tested chemical is placed on agar the chemical will diffuse from the disc into the agar. This diffusion will place the chemical in the agar only around the disc. The solubility of the chemical and its molecular size will determine the size of the area of chemical infiltration around the disc. If an organism is placed on the agar it will not grow in the area around the disc if it is susceptible to the chemical. This area of no growth around the disc is known as a "Zone of inhibition" or "Clear zone". For the disc diffusion, the zone diameters were measured with slipping calipers of the National for Clinical Laboratory Standers [44]. Agar-based methods such as Etest disk diffusion can be good alternatives because they are simpler and faster than broth methods [48, 49].

RESULTS AND DISCUSSION

The color, physical characteristic, micro-analytical data, molar conductance measurements of Cu(II), Co(II), Fe(II) and Mn(II) urea complexes are given in Table 1. The elemental analysis data of some prepared complexes revealed 1:4 molar ratio (M:U) (where M= Cu(II), Co(II), Fe(II) and Mn(II) and U= urea) are in a good agreement with the general formulas $\text{CuCl}_2 \cdot 2\text{U} \cdot 4\text{H}_2\text{O}$ (1), $\text{Co}(\text{NO}_3)_2 \cdot 6\text{U}$ (3), $\text{FeCl}_2 \cdot 6\text{U} \cdot 3\text{H}_2\text{O}$ (5) and $\text{MnCl}_2 \cdot 3\text{U} \cdot 3\text{H}_2\text{O}$ (7), on one hand and $\text{CuCl}_2 \cdot 2\text{U} \cdot 2\text{H}_2\text{O}$ (2), $\text{Co}(\text{NO}_3)_2 \cdot 2\text{U} \cdot 4\text{H}_2\text{O}$ (4), $\text{FeCl}_2 \cdot 3\text{U} \cdot 5\text{H}_2\text{O}$ (6) and $\text{MnCl}_2 \cdot 6\text{U}$ (8), complexes, on the other hand, prepared at room temperature and 60 °C respectively. The reactions can be represented by the stoichiometric equations:



The complexes are air-stable, hygroscopic, with low melting points, soluble in H₂O and dimethylformamide, DMF. The molar conductivities of (0.01g per 5 ml) the prepared complexes in DMF (Table 2) indicate that the complexes have an electrolytic nature.

3-1- Molar conductance measurements

The molar conductivity values for the urea complexes in DMF solvent are exhibited in the range of (95–3910) $\Omega^{-1} \text{ cm}^2 \text{ mol}^{-1}$, suggesting them to be electrolytes (Table 2). Conductivity measurements have frequently been used in structural of metal complexes (mode of coordination) within the limits of their solubility. They provide a method of testing the degree of ionization of the complexes, the molar ions that a complex liberates in solution (in case of presence anions outside the coordination sphere), the higher will be its molar conductivity and vice versa. It is clear from the conductivity data that the complexes present seem to be electrolytes. Also the molar conductance values indicate that the anions present outside the coordination sphere. This result was confirmed from the elemental analysis data where Cl^- or NO_3^- ions are precipitated with colored solution by adding of AgNO_3 or FeSO_4 solutions, respectively, this experimental test is a good matched with CHN data. All these complexes have electrolytic properties. This fact elucidated that the Cl^- or NO_3^- are present. These results establish the stoichiometry of these complexes, which are in agreement with the general formulas were suggested.

3-2- Magnetic measurements electron spin resonance

Magnetic measurements were carried out on a Sherwood Scientific magnetic balance according to the Gauy method. The calculations were evaluated by applying the following equations:

$$\chi_g = \frac{cl(R - R_o)}{10^9 M}$$

$$\chi_m = \chi_g MWt.$$

$$\mu_{eff} = 2.828 \sqrt{\chi_m T}$$

where χ is mass susceptibility per gm sample
 c is the calibration constant of the instrument and equal to 0.0816
 R is the balance reading for the sample and tube
 R_o is the balance reading for the empty tube
 M is the weight of the sample in gm
 T is the absolute temperature

The magnetic moments of the $\text{CuCl}_2 \cdot 2\text{U} \cdot 4\text{H}_2\text{O}$ (**1**) and $\text{CuCl}_2 \cdot 2\text{U} \cdot 2\text{H}_2\text{O}$ (**2**) complexes at $T = 300 \text{ K}$ and their corresponding hybrid orbitals were calculated. The observed values of the effective magnetic moments μ_{eff} measured for these complexes equal to 2.38 B.M and 1.96 respectively this is convenient with experimental values of 1.96 B.M. [50] obtained for octahedral Cu(II) complex with sp^3d^2 hyperdization for both Cu(II) complexes.

The ESR tool of analysis is useful in discuss the geometry and state of electrons in metal ion of the complexes. In this paper, the ESR spectrum of the Cu(II) complex was analyzed. The solid-state ESR spectra of some of the complexes exhibit axially symmetric g-tensor parameters with $g_{\parallel} > g_{\perp} > 2.0023$, indicating that the copper site has a $d_{x^2-y^2}$ ground-state characteristic of tetrahedral, square-planar, or octahedral stereochemistry. The $g_{\parallel} > g_{\perp}$ for synthesized Cu(II) urea complexes **1** and **2**, indicates a distorted octahedral geometry. ESR spectrum show splitting, this interpretive according to the interaction between two electrons (copper metal) and urea ligand because of the location of electrons on different sites.

3-3- Infrared spectra

The infrared spectra of the Cu(II), Co(II), Fe(II) and Mn(II) urea complexes at room temperature and 60°C are shown in Figs. 1 and 2 respectively. The band locations were measured for the mentioned urea complexes, together with the proposed assignments for the most characteristic vibrations are presented in Tables 3, 4, 5 and 6. In order to facilitate the spectroscopic analysis and to put our hand on the proper structure of the prepared complexes, the spectra of the urea complexes were accurately compared with those of the urea and similar complexes in literature. The discussion of the spectra will be addressed on the basis of the most characteristic vibrations.

The assignments of full vibrational analysis of crystalline urea have been published [38]. Tables from 3 to 6 give diagnostic infrared peaks of the free urea ligand, published work and Cu(II), Co(II), Fe(II) and Mn(II) complexes. Assignments have been given in comparison with the data obtained for the free urea, that is, uncoordinated, U [38] and its $[\text{Pt}(\text{urea})_2\text{Cl}_2]$ and $[\text{Cr}(\text{urea})_6]\text{Cl}_3$ complexes [38]. The effect of the coordination on the spectra of the complexes of urea with $[\text{Pt}(\text{urea})_2\text{Cl}_2]$ and $[\text{Cr}(\text{urea})_6]\text{Cl}_3$ complexes in which the coordination occurs through nitrogen and oxygen atoms, respectively [38]. The mode of coordination of urea with metal ions seems to be dependent upon the type and nature of metal. Pt(II) ions in $[\text{Pt}(\text{urea})_2\text{Cl}_2]$ coordinate to the nitrogen, whereas Fe(III),

Zn(II), and Cu(II) coordinate to the oxygen of urea [38]. For all the prepared complexes, the coordination mode take place *via* oxygen of amide group, the positively charged metal ion stabilizes the negative charge on the oxygen atom; the NCO group now occurs in its polar resonance form and the double bond character of the CN bond increases or still not affected, while the double bond character of the CO bond decreases, resulting in an increase of the CN stretching frequency with a simultaneous decrease in the CO stretching frequency [52, 53]. The IR-active $\nu(\text{M}-\text{O})$ vibration of all prepared urea complexes is observed at the range (546- 452) cm^{-1} [52, 53].

The band related to the stretching vibration $\nu(\text{O}-\text{H})$ of uncoordinated H_2O is observed as expected in the range of (3420-3450) cm^{-1} , while the corresponding bending motion of the uncoordinated water, $\delta(\text{H}_2\text{O})$, is observed in the range of (1630-1638) cm^{-1} .

In both cobalt complexes, the characteristic stretching vibrations of the nitrate group, NO_3^- , is observed at around (1385 and 1159 cm^{-1} attributed to $\nu_{\text{as}}(\text{NO}_2)$ and $\nu_{\text{s}}(\text{NO}_2)$, respectively [54]. The stretching motion of ($\nu(\text{N}=\text{O})$) is observed at 1477 cm^{-1} as a strong band, while the bending motion of the type $\delta(\text{NO}_2)$ are well resolved and observed at 784 as a medium band.

3-4- Thermal analysis

The $\text{CuCl}_2 \cdot 2\text{U} \cdot 4\text{H}_2\text{O}$ (1) and $\text{CuCl}_2 \cdot 2\text{U} \cdot 2\text{H}_2\text{O}$ (2) $\text{Co}(\text{NO}_3)_2 \cdot 6\text{U}$ (3) and $\text{Co}(\text{NO}_3)_2 \cdot 2\text{U} \cdot 4\text{H}_2\text{O}$ (4) $\text{FeCl}_2 \cdot 6\text{U} \cdot 3\text{H}_2\text{O}$ (5) and $\text{FeCl}_2 \cdot 3\text{U} \cdot 5\text{H}_2\text{O}$ (6) $\text{MnCl}_2 \cdot 3\text{U} \cdot 3\text{H}_2\text{O}$ (7) and $\text{MnCl}_2 \cdot 6\text{U}$ (8) complexes were studied by thermogravimetric analysis from ambient temperature to 800 °C in oxygen atmosphere. Figures 3 and 4 and Tables (7 and 8) illustrate TG curves and decomposition stages obtained for these complexes with a temperature rate 30 °C/min.

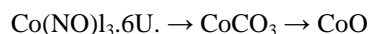
Thermal analysis of $\text{CuCl}_2 \cdot 2\text{U} \cdot 4\text{H}_2\text{O}$ (1) complex, Fig. 3(1), shows that copper (II) complex prepared at room temperature is thermally stable up to 139 °C. Its thermal decomposition occurs in three stages of weight loss of different intermediates followed by three endothermic maximum temperatures $\text{DTG}_{\text{max}} = 235, 364, \text{ and } 608$ °C, respectively. From the TG-DTG curves it is clear that the first decomposition stage from 139 to 284 °C corresponded to the loss of four moles of water (22.90% experimental loss; 22.05% theoretical loss). The continued loss in the second step corresponding to two moles of urea after trapping $\frac{1}{2}\text{O}_2$ from air, the experimental loss of this step is 41.893% while the theoretical loss is 41.656%. The last step shows the liberation of one mol of Cl_2 (experimental loss; 21.541%, theoretical loss 21.747%) leaving copper as a residue. The most probable thermal decomposition of the complex may be represented as:



The TG curve of $\text{CuCl}_2 \cdot 2\text{U} \cdot 2\text{H}_2\text{O}$ (2) complex is shown in Fig. 4(2). Three stages of dissociation of the complex are indicated in TG and DTG curve. The first decomposition starts at 98 °C and ends at 245 °C, with an experimental mass loss of 22.977% against a theoretical loss of 23.410%, corresponding to the release of 2 moles of water and one hydrazine molecule forming unstable $\text{Cu} \cdot \text{CO} \cdot \text{U} \cdot \text{Cl}_2$ complex. The second stage takes place between 245 and 399 °C, with with maximum peak at 323 °C and experimental mass loss of 8.593% against a theoretical loss of 9.639%, corresponding to the release CO . The third stage is from 468 to 635 °C with maximum peak at 548 °C, the experimental mass loss is 19.904% against a theoretical mass loss of 20.655%, due to the dissociation of 1 mol of urea, leaving anhydrous CuCl_2 . The mechanism of the thermal decomposition of the complex is proposed as:



The TG curve of $\text{Co}(\text{NO}_3)_2 \cdot 6\text{U}$ (3) complex is shown in Fig. 3(3). The TG-DTG curve indicates the dissociation of the complex in two stages. The first transition changes from 172 to 288 °C, with an experimental mass loss of 78.187% against a theoretical mass loss of 78.080%, corresponding to the release of five urea molecules and two moles nitrate groups. The second transformation is from 428 to 477 °C, with an experimental and theoretical mass losses of 6.991%, and 8.103% respectively due to the release of one mol of carbon dioxide, leaving CoO as a residue, the mechanism of the thermal decomposition of the complex is proposed as:



The TG-DTG curve of $\text{Co}(\text{NO}_3)_2 \cdot 2\text{U} \cdot 4\text{H}_2\text{O}$ (4) complex is shown in Fig. 4(4). Two stages of transition are observed in the TG-DTG curve. The first transition is from 40 °C to 218 °C with $\text{DTG}_{\text{max}} = 126$ °C, with an experimental mass loss of 5.145% against a theoretical loss of 4.799%, corresponding to the release of 1 mol of water. The second transition stage started from 183 °C to 462 °C, with DTG_{max} at 273, °C, the experimental mass loss this stage 75.30% against a theoretical mass loss of 74.66%, this is due to the release of 2 mol of urea, 3 mol

water, 2 nitrate ions and trapping of $\frac{1}{2}$ O₂ from air forming CoO. The sequential thermal dissociation process of the complex can be shown as follows:



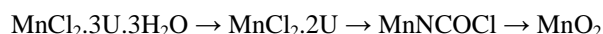
The TG-DTG curve of FeCl₂·6U·3H₂O (5) complex is shown in Fig. 3(5). Four stages of transitions are observed in the TG-DTG curve. The first transition changes from 42 °C to 159 °C with DTG_{max} = 54 °C, with an experimental mass loss of 4.135% against a theoretical loss of 3.328%, corresponding to the release of 1 mol of water. The second transition changes from 159 °C to 290 °C with DTG_{max} = 243 °C, with an experimental mass loss of 45.382% against a theoretical loss of 46.9708%, corresponding to the release of 2 mol of water, 2 mol of ammonium chloride, 3 mol of ammonia, 1 mol of hydrazine and 1 mol of N₂. The third transition is from 290 °C to 397 °C with DTG_{max} = 351 °C and an experimental mass loss of 32.033% against a theoretical loss of 32.00%, corresponding to the release of 1 mol cyanuric acid and 1 mol carbon dioxide. In the final transition 1 mol carbon monoxide is released this takes place between 397 °C and 642 °C with DTG_{max} at 417 °C (3.60% experimental loss; 5.18% theoretical loss). The thermal decomposition of the above complex can be represented



The TG curve of FeCl₂·3U·5H₂O (6) complex is shown in Fig. 4(6). Three stages of dissociation of the complex are indicated in TG and DTG curve. The first decomposition starts at 40 °C and ends at 170 °C, with an experimental mass loss of 6.856% against a theoretical loss of 6.804%, corresponds to the release of 1.5 moles of water. The second decomposition takes place between 170 and 285 °C, with with maximum peak at 238 °C and experimental mass loss of 46.491% against a theoretical loss of 46.119%, corresponding to the release of 3.5 mol of water and 2 mol Urea. The third stage is from 285 to 425 °C with maximum peak at 370 °C, the experimental mass loss is 27.955% against a theoretical mass loss of 28.98%, corresponding to the dissociation of 1 mol of HCN, 2mol HCl, $\frac{1}{2}$ mol N₂, $\frac{1}{2}$ mol H₂. The mechanism of the thermal decomposition of the complex is proposed as:



The TG curve for MnCl₂·3U·3H₂O (7) complex, Fig. 3(7), has three stages of mass losses within the temperature range 156-624 °C at 267, 387 and 480 °C DTG maximum peaks. The first stage is between 156-325 °C and with experimental mass loss of 39.858% against a theoretical mass loss of 40.286%, corresponding to the loss of 3 moles water and 1 mol of urea. The second stage is between 325-432 °C with an experimental and theoretical mass losses of 11.929% and 12.387%, respectively, is due to the loss of 1 mol of ammonium chloride. The third stage of decomposition at the temperature range 432-624 °C is assigned to the loss of $\frac{1}{2}$ Cl₂ and 1 CN with an experimental mass loss of 13.534% and a theoretical mass loss of 14.239%, leaving MnO₂ as a result of trapping $\frac{1}{2}$ O₂ from air. The proposed thermal decomposition mechanism of the complex can be given as:



The MnCl₂·6U (8) complex, Fig. 4(8) shows two main stages of decomposition as evident from DTG maximum peaks at 260 °C and 466 °C. The first stage of decomposition with an experimental mass loss of 41.272% and a theoretical mass loss 41.405% is assigned to the decomposition of 7 mol NH₃, 3mol CO₂ and 1 mol N₂. The second stage, which has an experimental mass loss of 20.797% is in good agreement with theoretical mass loss of 20.989%, is attributed to the loss of C₂H₃N₃O₃ leaving MnCl₂ and residual carbon. The proposed thermal decomposition mechanism of the complex can be given as:



3-6- X- ray powder diffraction studies

The x-ray powder diffraction patterns for the Cu(II), Co(II), Fe(III) and Mn(II) urea complexes at different temperatures with formulas; CuCl₂·2U·4H₂O (1) and CuCl₂·2U·2H₂O (2) Co(NO₃)₂·6U (3) and Co(NO₃)₂·2U·4H₂O (4) FeCl₂·6U·3H₂O (5) and FeCl₂·3U·5H₂O (6) MnCl₂·3U·3H₂O (7) and MnCl₂·6U (8) are depicted in Figs. 5 and 6. Inspecting these patterns, we notice that all systems are well crystalline. The crystallite size of these complexes could be estimated from XRD patterns by applying FWHM of the characteristic peaks using Deby-Scherrer equation 1 [55]. Where D is the particle size of the crystal grain, K is a constant (0.94 for Cu grid), λ is the x-ray wavelength (1.5406 Å), θ is the Bragg diffraction angle and β is the integral peak width. The particle size was estimated according to the highest value of intensity compared with the other peaks. These data gave an impression that the particle size located within nano scale range.

$$D = K\lambda/\beta \cos\theta \quad (1)$$

3-7- SEM and EDX studies

Scanning electron microscopy is a simple tool used to give an impression about the microscopic aspects of the physical behavior of urea as a chelating agent (Fig. 7 and 8). Although this tool is not a qualified method to confirm complex formation but it can be a reference to the presence of a single component in the synthetic complexes. The pictures of the Ag(I), Cr(III), Cd(II) and Zn(II) complexes show a small particle size with a nano feature products. The chemical analysis results by EDX for the formed complexes show a homogenous distribution in between metal ions and chelating agent. SEM examinations were checked the morphology of the surfaces of these complexes that show small particles which tendency to agglomerates formation with different shapes comparison with the start materials. The peaks of EDX profile of these complexes (Fig. 9 and 10) refer to all elements which constitute the molecules of urea complexes (1- 8) that clearly identified confirming the proposed structures.

3-8- Biological evaluation

Biological evaluations were checked in term of antimicrobial activities of target compounds against gram-positive (*Bacillus subtilis* and *Staphylococcus aureus*) and gram-negative (*Escherichia coli* and *Pseudomonas aeruginosa*) and tow strains of fungus (*Aspergillus flavus* and *Candida albicans*). Result from the agar disc diffusion tests for antimicrobial activities of target compounds are presented in Table 9, and illustrated in Fig. 11. The diameters of zone of inhibition (in mm) of the standard drug tetracycline against gram positive bacteria *B. subtilis* and *S. aureus* and gram negative bacteria *E. coli* and *P. aeruginosa* were found to be 36, 30, 31 and 35 mm, respectively, while the standard drug amphotericin B against *Aspergillus flavus* and *Candida albicans* gave 18 and 19, respectively. Under identical conditions, Table 9 shows that, complex **1** has (12, 12, 12, 11, 10 and 10 mm), complex **3** has (22, 22, 24, 20, 14 and 19 mm), complex **5** has (14, 12, 14, 18, 10 and 14 mm), and complex **7** has (10, 10, 10, 0.0, 0.0 and 0.0 mm), respectively, for *Bacillus subtilis*, *Escherichia coli*, *Pseudomonas aeruginosa*, *Staphylococcus aureus*, *Aspergillus flavus* and *Candida albicans*. All complexes were found to be efficient antimicrobial agents. except for complex **7** which has no efficiency against *Staphylococcus aureus*, *Aspergillus flavus* and *Candida albicans* fungus.

Table 1: Physical characterization, micro-analytical data of urea complexes

Complexes Molecular formula Empirical formula (MW.)	Color	Molar ratio	Elemental analysis (%) Found (Calcd.)	
			C	H
CuCl ₂ .2U.4H ₂ O (1) 326.48 g/mol	Light green	1:4	07.30 (07.35)	04.14 (04.90)
CuCl ₂ .2U.2H ₂ O (2) 290.48 g/mol	Green	1:4	08.50 (08.26)	04.40 (04.13)
CO(NO ₃) ₂ .6U (3), 543.03 g/mol	Dark red	1:4	13.50 (13.26)	04.20 (04.42)
CO(NO ₃) ₂ .2U.4H ₂ O (4) 375.03 g/mol	Red purple	1:4	06.43 (06.40)	04.70 (04.27)
FeCl ₂ .6U.3H ₂ O (5), 540.8 g/mol	Yellow	1:4	12.40 (13.33)	02.40 (04.81)
FeCl ₂ .3U.5H ₂ O (6) 396.8 g/mol	Broun	1:4	08.84 (09.08)	04.70 (04.54)
MnCl ₂ .3U.3H ₂ O (7) 431.91 g/mol	White creamy	1:4	07.50 (08.34)	04.30 (04.18)
MnCl ₂ .6U. (8) 557.91 g/mol	White	1:4	11.70 (12.90)	04.60 (04.30)

Table 2: Molar conductance and magnetic moment data of urea complexes

Complex	Δm ($\Omega^{-1} \text{cm}^2 \text{mol}^{-1}$)	μ_{eff}
CuCl ₂ .2U.4H ₂ O (1)	340	2.38
CuCl ₂ .2U.2H ₂ O (2)	-	1.69
CO(NO ₃) ₂ .6U (3),	3910	2.43
CO(NO ₃) ₂ .2U.4H ₂ O (4)	-	2.42
FeCl ₂ .6U.3H ₂ O (5),	946	2.95
FeCl ₂ .3U.5H ₂ O (6)	-	2.91
MnCl ₂ .3U.3H ₂ O (7)	95	2.73
MnCl ₂ .6U. (8)	-	6.17

Table 3: Characteristic infrared frequencies (cm⁻¹) and tentative assignments of urea (U), [Pt(urea)₂Cl₂] (A), [Cr(urea)₆]Cl₃ (B), CuCl₂·2U·4H₂O (1) and CuCl₂·2U·2H₂O (2) complexes

U	A	B	1	2	Assignments ^(b)
3450	3390	3440	3450	3446	v _{as} (NH ₂)
	3290	3330	3347	3354	v(OH); H ₂ O
3350	3130 3030	3190	2362	3316	v _s (NH ₂)
1683	1725	1505	1628	1622	δ(C=O)
1471	1395	1505	1464	1403	v(C-N)

Table 4: Characteristic infrared frequencies (cm⁻¹) and tentative assignments of urea (U), [Pt(urea)₂Cl₂] (A), [Cr(urea)₆]Cl₃ (B), Co(NO₃)₂·6U(3) and Co(NO₃)₂·2U·4H₂O (4) complexes

U	A	B	3	4	Assignments ^(b)
3450	3390	3440	3459	3450	v(OH); H ₂ O
	3290	3330	3346	3353	v _{as} (NH ₂)
3350	3130 3030	3190	2362	3212	v _s (NH ₂)
1683	1725	1505	1561	1564	δ(H ₂ O) δ(C=O)
1471	1395	1505	1477	1477	v(C-N)

Table 5: Characteristic infrared frequencies (cm⁻¹) and tentative assignments of urea (U), [Pt(urea)₂Cl₂] (A), [Cr(urea)₆]Cl₃ (B), FeCl₂·6U·3H₂O (5) and FeCl₂·U·H₂O (6) complexes

U	A	B	5	6	Assignments ^(b)
3450	3390	3440	3450	3448	v(OH); H ₂ O
	3290	3330	3346	3358	v _{as} (NH ₂)
3350	3130 3030	3190	3202	3198	v _s (NH ₂)
1683	1725	1505	1630	1630	δ(C=O)
1471	1395	1505	1495	1402	v(C-N)

Table 6: Characteristic infrared frequencies (cm⁻¹) and tentative assignments of urea (U), [Pt(urea)₂Cl₂] (A), [Cr(urea)₆]Cl₃ (B), MnCl₂·3U·3H₂O (7) and MnCl₂·6U (8) complexes

U	A	B	7	8	Assignments ^(b)
3450	3390	3440	3464	3437	v(OH); H ₂ O
	3290	3330	3354	3350	v _{as} (NH ₂)
3350	3130 3030	3190	3219	---	v _s (NH ₂)
1683	1725	1505	1658	1656	δ(C=O) δ(H ₂ O)
1471	1395	1505	1496	1473	v(C-N)

Table 7: The maximum temperature, T_{max}/°C, and weight loss values of the decomposition stages for the CuCl₂·2U·4H₂O (1), Co(NO₃)₂·6U(3), FeCl₂·6U·3H₂O (5), and MnCl₂·3U·3H₂O (7) complexes

Complexes	Decomposition	T _{max} /°C	Lost Species	% Weight loss	
				Found	Calc.
1	First step	235	4H ₂ O	22.903	22.053
	Second step	364	2NH ₃ +H ₂ O+N ₂ +2CO ₂	41.983	41.656
	Third step	607	Cl ₂	21.541	21.747
	Residue		Cu metal	19.450	14.547
3	First step	270	5CO+2NO ₂ +6N ₂ H ₄	78.187	78.080
	Second step	477	CO ₂	6.991	8.102
	Residue		CoO	13.793	13.818
5	First step	54	H ₂ O	4.135	3.328
	Second step	243	2H ₂ O+2NH ₄ Cl+3NH ₃ +N ₂ H ₄ +N ₂	45.382	46.970
	Third step	351	C ₃ H ₃ N ₃ O ₃ +CO ₂	32.00	32.033
	Forth step	417	CO	3.600	5.180
	Residue		FeO	13.314	12.489
7	First step	267	4NH ₃ +2CO ₂ +H ₂ O	39.585	40.286
	Second step	387	NH ₄ Cl	11.929	12.387
	Third step	480	½Cl ₂ +CN	13.534	14.239
	Residue		MnO ₂	20.129	---

Table 8: The maximum temperature, $T_{max}/^{\circ}C$, and weight loss values of the decomposition stages for the $CuCl_2 \cdot 2U \cdot 2H_2O$ (2), $Co(NO_3)_2 \cdot 2U \cdot 4H_2O$ (4), $FeCl_2 \cdot 3U \cdot 5H_2O$ (6) and $MnCl_2 \cdot 6U$ (8) complexes

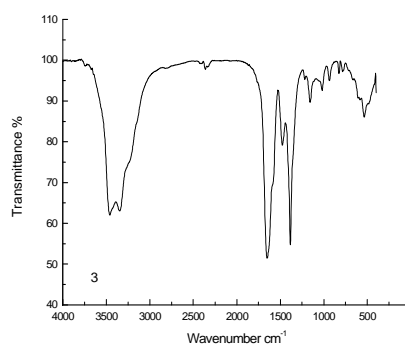
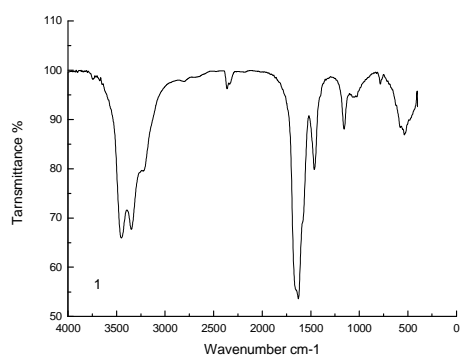
Complexes	Decomposition	$T_{max}/^{\circ}C$	Lost Species	% Weight loss	
				Found	Calc.
2	First step	154	$2H_2O + N_2H_4$	22.977	23.41
	Second step	323	CO	8.593	9.639
	Third step	548	Urea	19.904	20.655
	Residue		$CuCl_2$	46.303	46.296
4	First step	126	H_2O	5.145	4.799
	Second step	293	$H_2O + 4NH_3 + 2CO_2 + 2NO_2 + \frac{1}{2}O_2$	75.305	75.194
	Residue		CoO	19.981	20.541
6	First step		$\frac{1}{2}H_2O$	6.856	6.804
	Second step	238	$3.5H_2O + 2Urea$	46.491	46.119
	Third step	370	$HCN + 2HCl + \frac{1}{2}N_2 + \frac{1}{2}H_2$	27.955	28.981
	Residue		FeO	18.145	18.096
8	First step	260	$7NH_3 + 3CO_2 + N_2$	41.276	41.405
	Second step	466	$C_2H_3N_3O_3$	20.778	20.989
	Residue		$MnCl_2 + Carbon$	22.573	---

Table 9: Inhibition zone diameter (mm) of the target compounds against tested microorganisms for $CuCl_2 \cdot 2U \cdot 4H_2O$ (1), $Co(NO_3)_2 \cdot 6U$ (3), $FeCl_2 \cdot 6U \cdot 3H_2O$ (5), and $MnCl_2 \cdot 3U \cdot 3H_2O$ complexes

Sample	Inhibition zone diameter (mm / mg sample)					
	<i>Bacillus subtilis</i> (G ⁺)	<i>Escherichia coli</i> (G ⁻)	<i>Pseudomonas aeruginosa</i> (G ⁻)	<i>Staphylococcus aureus</i> (G ⁺)	<i>Aspergillus flavus</i> (Fungus)	<i>Candida albicans</i> (Fungus)
Control: DMSO	0.0	0.0	0.0	0.0	0.0	0.0
Standard Antibacterial agent (Tetracycline)	36	31	35	30	--	--
Standard Antifungal agent (Amphotericin B)	--	--	--	--	18	19
1	12	12	12	11	10	10
3	22	22	24	20	14	19
5	14	12	14	18	10	14
7	10	10	10	0.0	0.0	0.0

G: Gram reaction.

Solvent: DMSO.



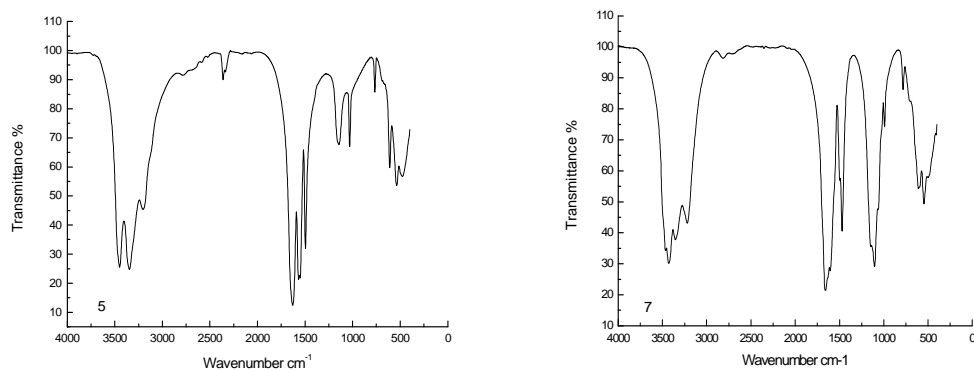


Fig. 1: Infrared spectra of urea complexes at room temperature: $\text{CuCl}_2 \cdot 2\text{U} \cdot 4\text{H}_2\text{O}$ (1), $\text{Co}(\text{NO}_3)_2 \cdot 6\text{U}$ (3), $\text{FeCl}_2 \cdot 6\text{U} \cdot 3\text{H}_2\text{O}$ (5) and $\text{MnCl}_2 \cdot 3\text{U} \cdot 3\text{H}_2\text{O}$ (7) complexes

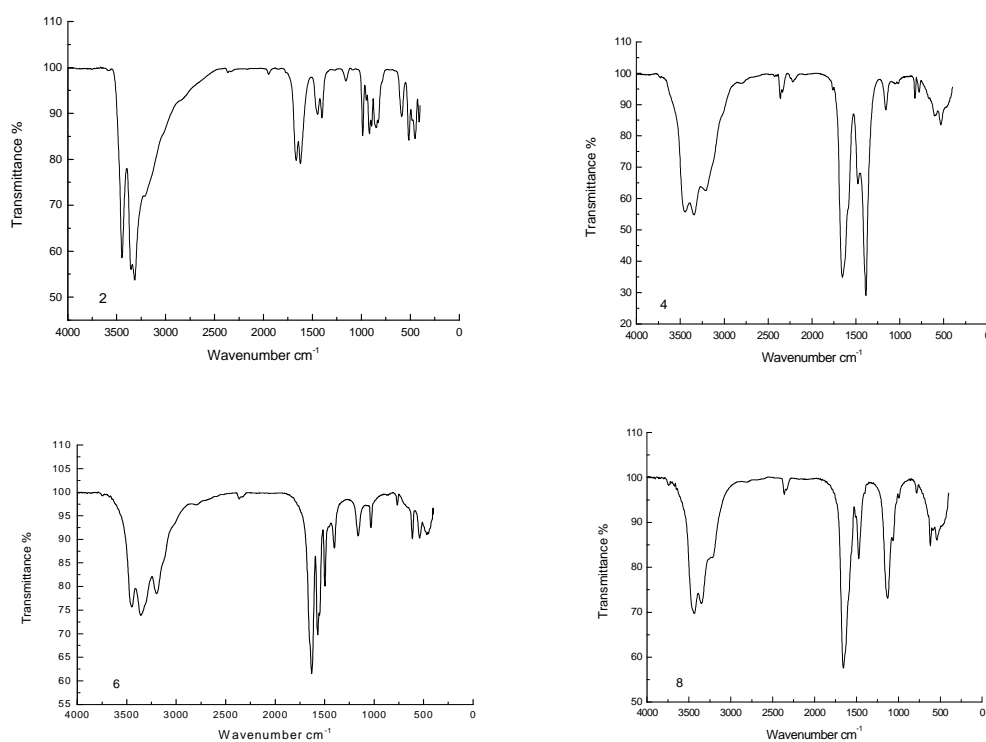
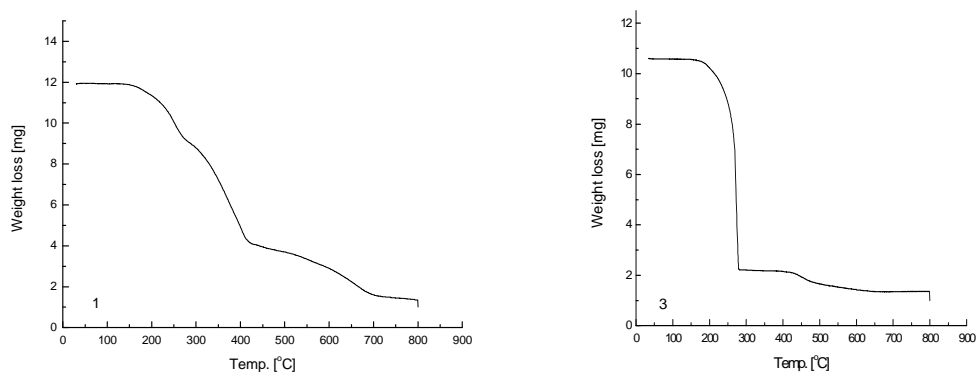


Fig. 2: Infrared spectra of urea complexes at 60 °C: $\text{CuCl}_2 \cdot 2\text{U} \cdot 2\text{H}_2\text{O}$ (2), $\text{Co}(\text{NO}_3)_2 \cdot 2\text{U} \cdot 4\text{H}_2\text{O}$ (4), $\text{FeCl}_2 \cdot 3\text{U} \cdot 5\text{H}_2\text{O}$ (6) and $\text{MnCl}_2 \cdot 6\text{U}$ (8) complexes



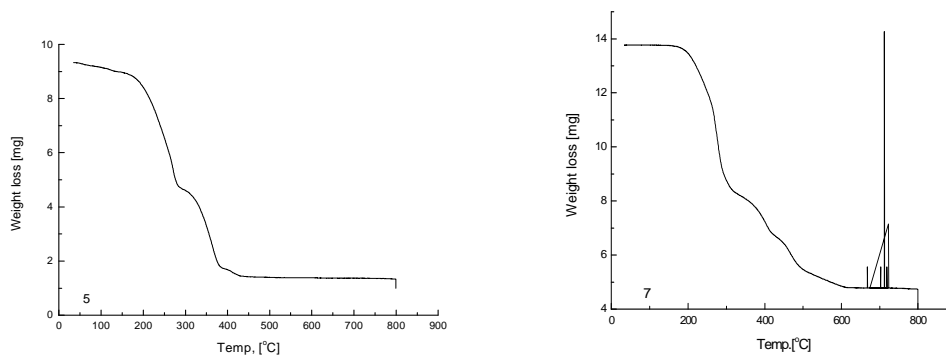


Fig. 3: TG curves of $\text{CuCl}_2 \cdot 2\text{U} \cdot 2\text{H}_2\text{O}$ (2), $\text{Co}(\text{NO}_3)_2 \cdot 2\text{U} \cdot 4\text{H}_2\text{O}$ (4), $\text{FeCl}_2 \cdot 3\text{U} \cdot 5\text{H}_2\text{O}$ (6) and $\text{MnCl}_2 \cdot 6\text{U}$ (8) complexes

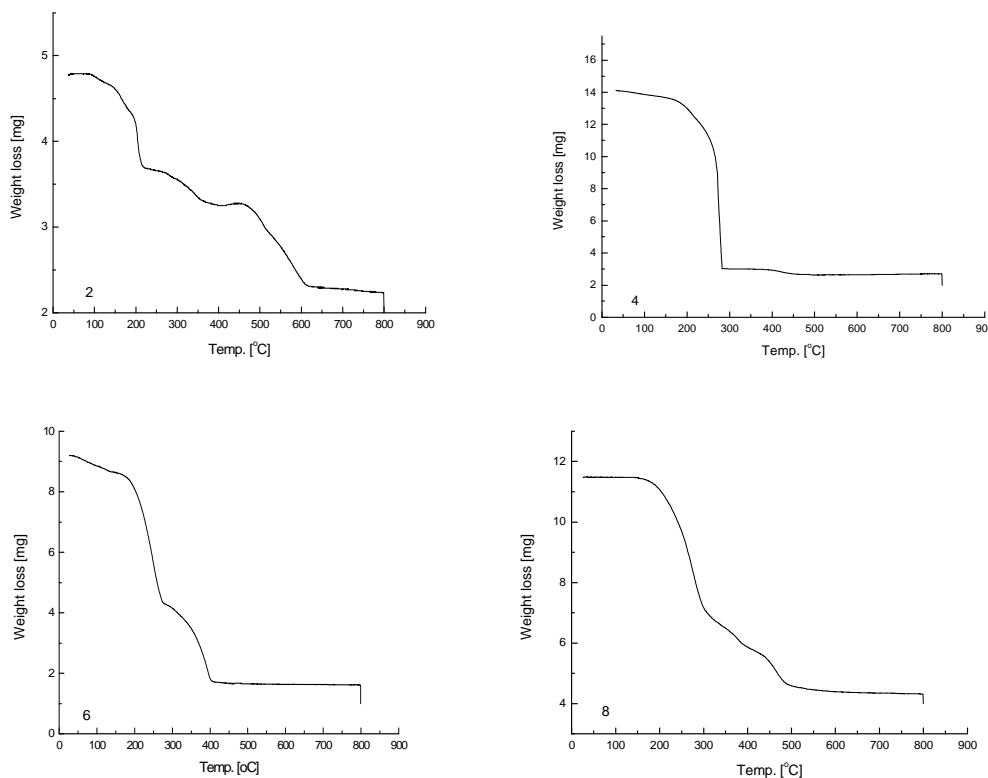
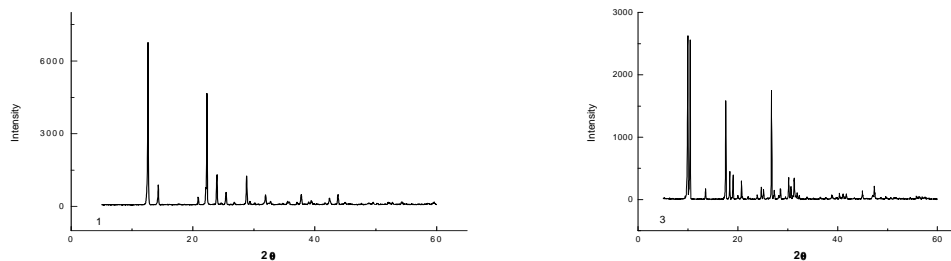


Fig. 4: TG curves of $\text{CuCl}_2 \cdot 2\text{U} \cdot 2\text{H}_2\text{O}$ (2), $\text{Co}(\text{NO}_3)_2 \cdot 2\text{U} \cdot 4\text{H}_2\text{O}$ (4), $\text{FeCl}_2 \cdot 3\text{U} \cdot 5\text{H}_2\text{O}$ (6) and $\text{MnCl}_2 \cdot 6\text{U}$ (8) complexes



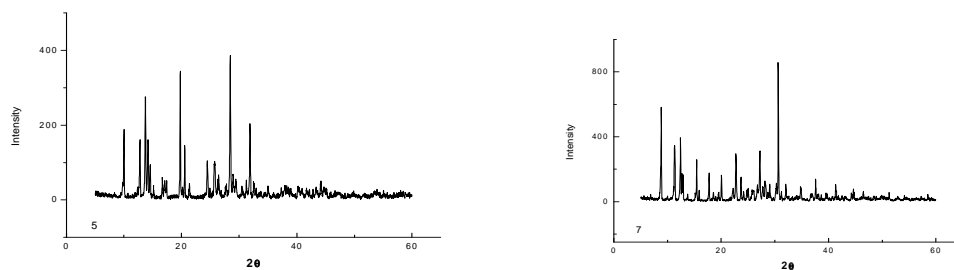


Fig. 5: XRD spectra of urea complexes at room temperature: $\text{CuCl}_2 \cdot 2\text{U} \cdot 4\text{H}_2\text{O}$ (1), $\text{Co}(\text{NO}_3)_2 \cdot 6\text{U}$ (3), $\text{FeCl}_2 \cdot 6\text{U} \cdot 3\text{H}_2\text{O}$ (5) and $\text{MnCl}_2 \cdot 3\text{U} \cdot 3\text{H}_2\text{O}$ (7) complexes

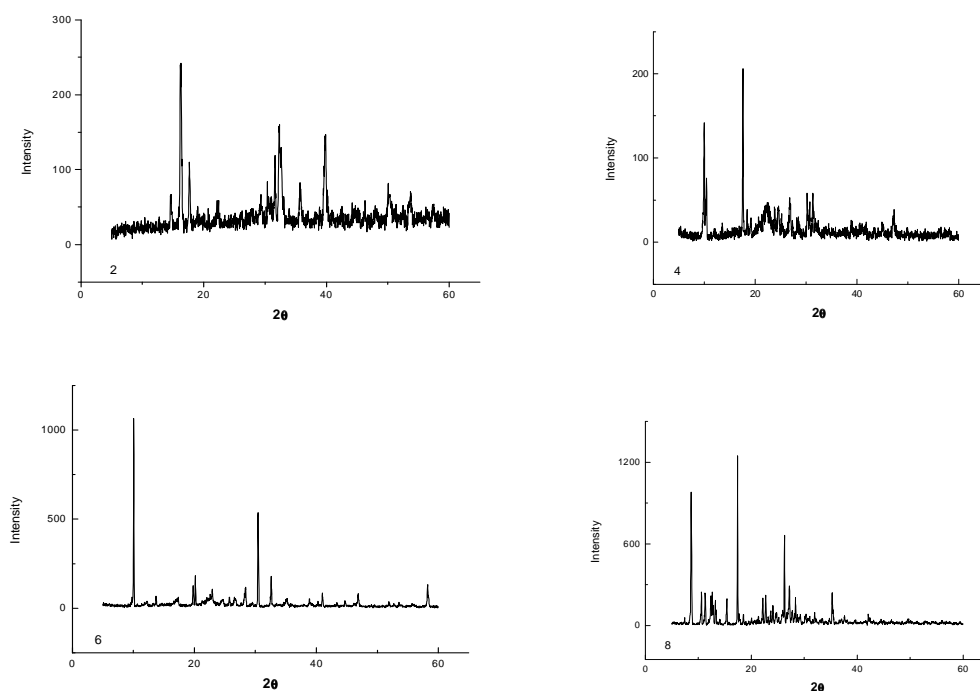


Fig. 6: XRD spectra of urea complexes at room temperature: $\text{CuCl}_2 \cdot 2\text{U} \cdot 4\text{H}_2\text{O}$ (1), $\text{Co}(\text{NO}_3)_2 \cdot 6\text{U}$ (3), $\text{FeCl}_2 \cdot 6\text{U} \cdot 3\text{H}_2\text{O}$ (5) and $\text{MnCl}_2 \cdot 3\text{U} \cdot 3\text{H}_2\text{O}$ (7) complexes

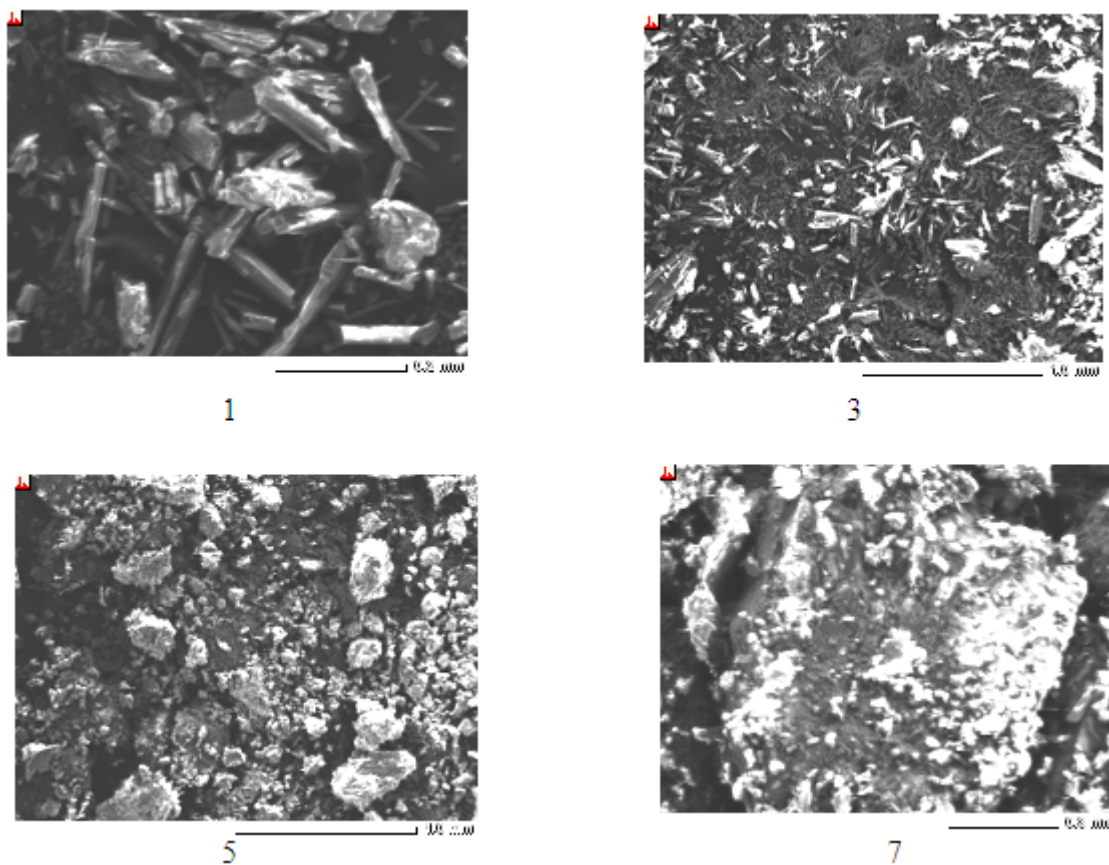


Fig. 7: SEM image of $\text{CuCl}_2 \cdot 2\text{U} \cdot 4\text{H}_2\text{O}$ (1), $\text{Co}(\text{NO}_3)_2 \cdot 6\text{U}$ (3), $\text{FeCl}_2 \cdot 6\text{U} \cdot 3\text{H}_2\text{O}$ (5) and $\text{MnCl}_2 \cdot 3\text{U} \cdot 3\text{H}_2\text{O}$ (7) complexes

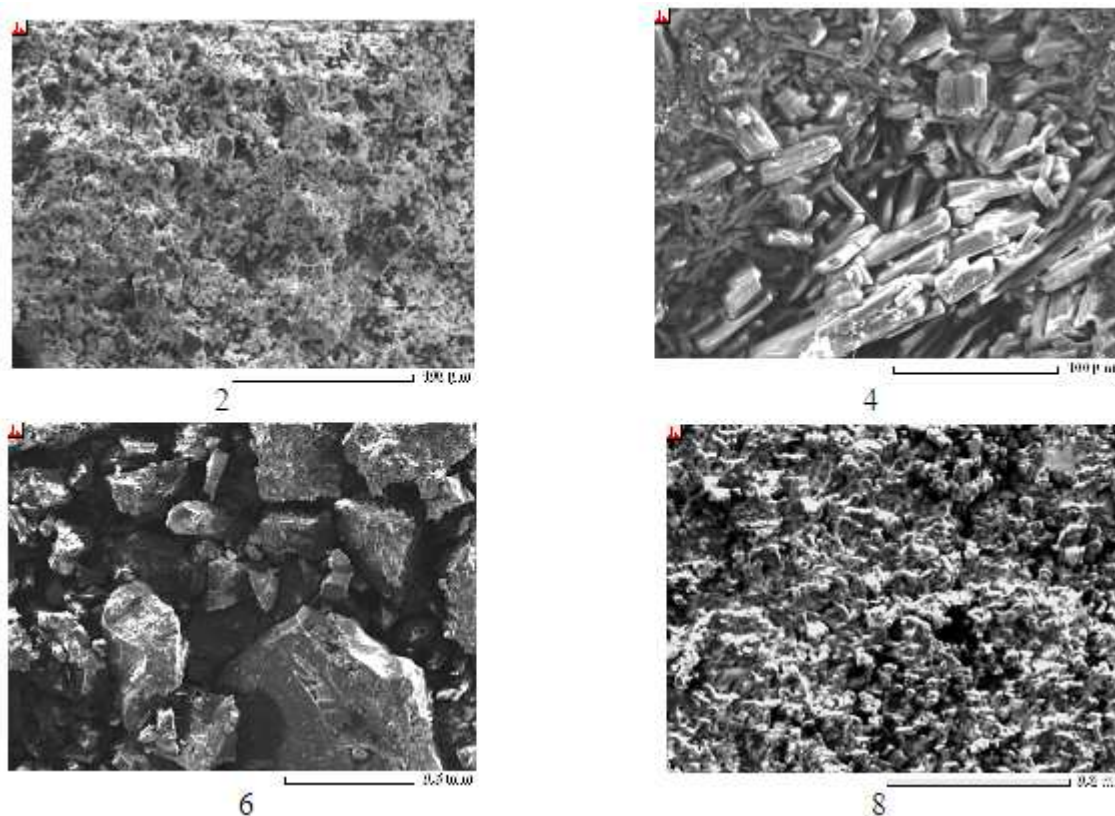


Fig. 8: SEM image of $\text{CuCl}_2 \cdot 2\text{U} \cdot 2\text{H}_2\text{O}$ (2), $\text{Co}(\text{NO}_3)_2 \cdot 2\text{U} \cdot 4\text{H}_2\text{O}$ (4), $\text{FeCl}_2 \cdot 3\text{U} \cdot 5\text{H}_2\text{O}$ (6) and $\text{MnCl}_2 \cdot 6\text{U}$ (8) complexes

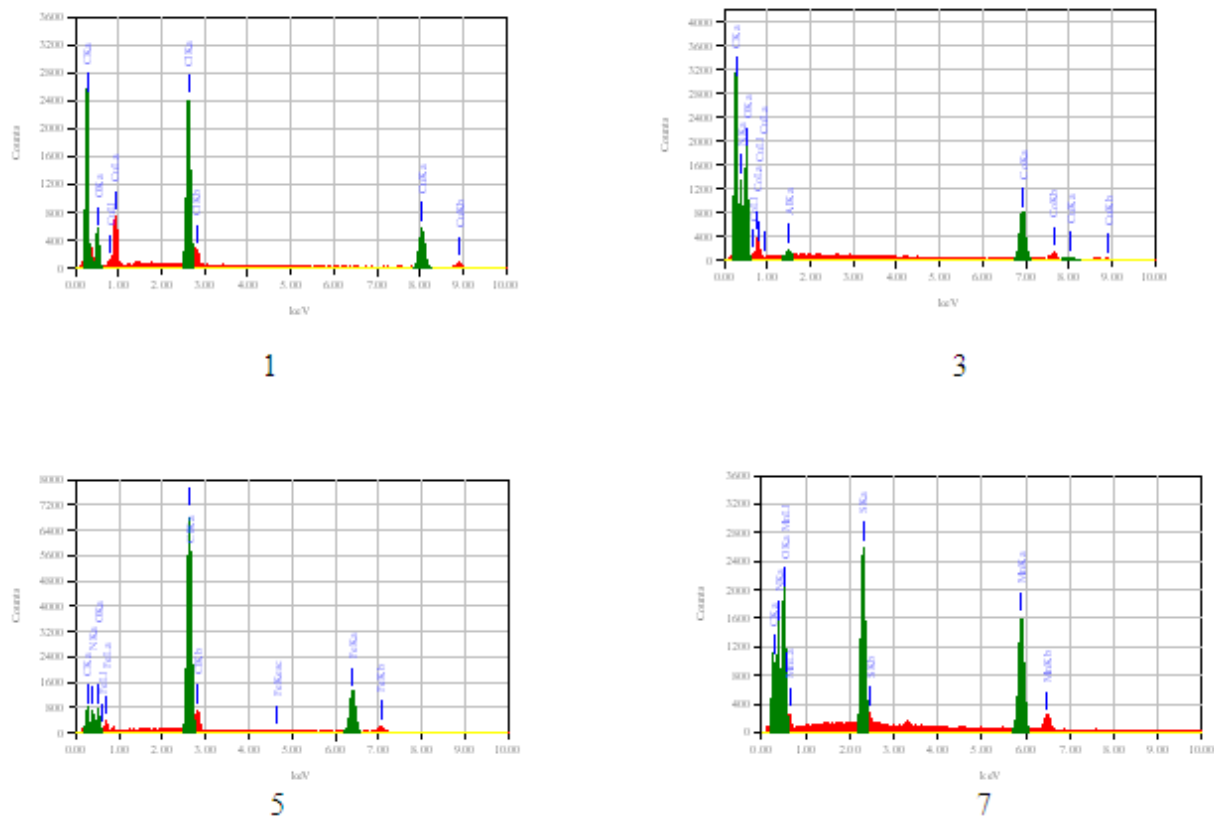


Fig. 9: EDX diagram of $\text{CuCl}_2 \cdot 2\text{U} \cdot 4\text{H}_2\text{O}$ (1), $\text{Co}(\text{NO}_3)_2 \cdot 6\text{U}$ (3), $\text{FeCl}_2 \cdot 6\text{U} \cdot 3\text{H}_2\text{O}$ (5) and $\text{MnCl}_2 \cdot 3\text{U} \cdot 3\text{H}_2\text{O}$ (7) complexes

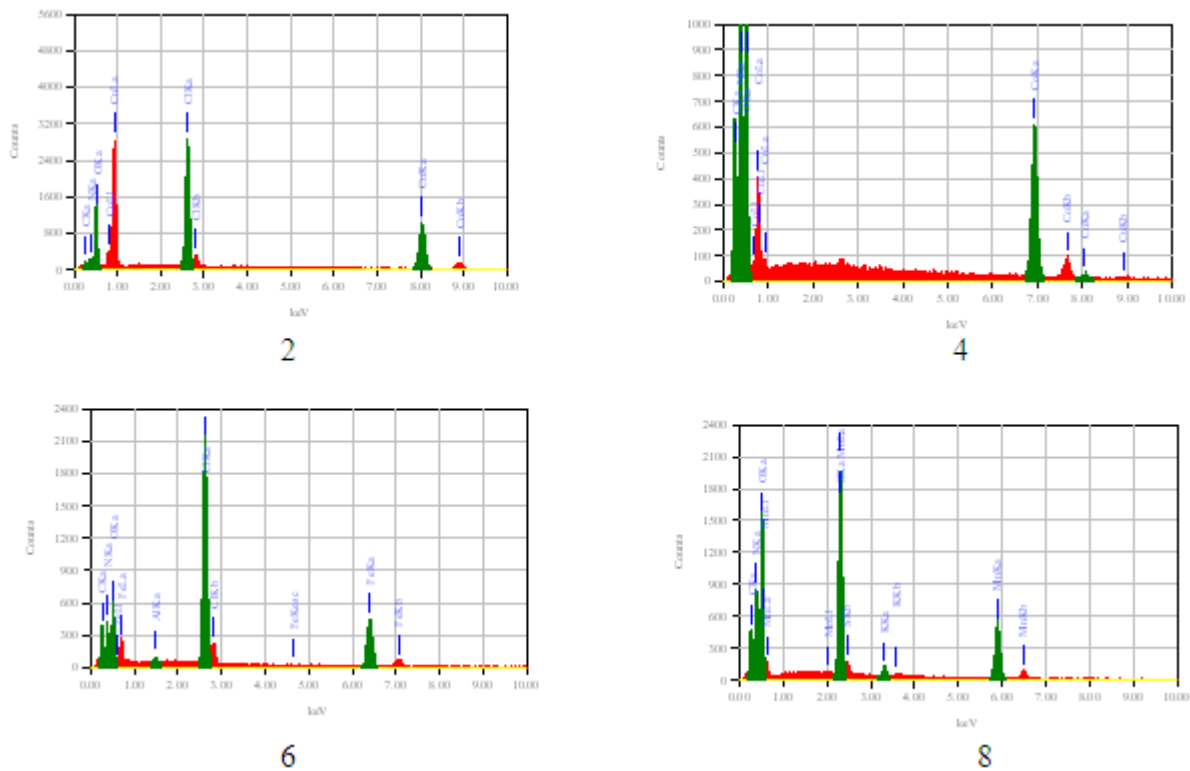


Fig. 10:EDX diagram of $\text{CuCl}_2 \cdot 2\text{U} \cdot 2\text{H}_2\text{O}$ (2), $\text{Co}(\text{NO}_3)_2 \cdot 2\text{U} \cdot 4\text{H}_2\text{O}$ (4), $\text{FeCl}_2 \cdot 3\text{U} \cdot 5\text{H}_2\text{O}$ (6) and $\text{MnCl}_2 \cdot 6\text{U}$ (8) complexes

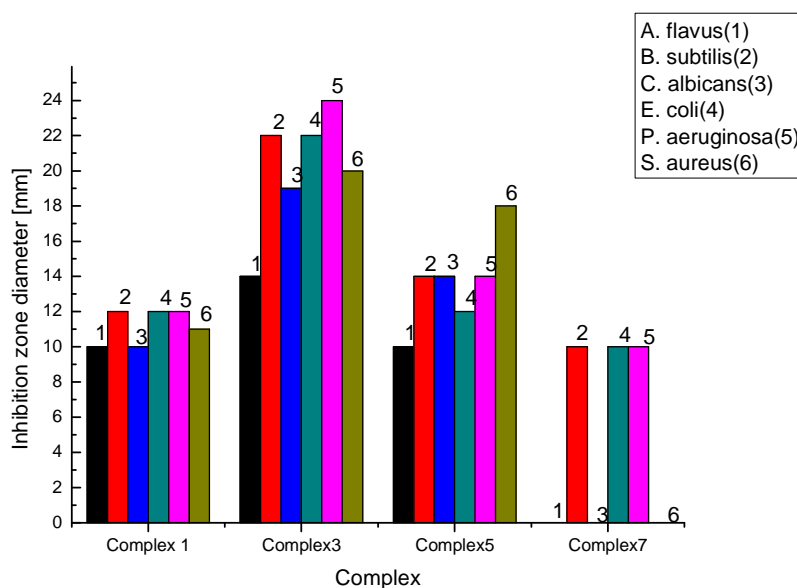


Fig.11: Biological evaluation of $\text{CuCl}_2 \cdot 2\text{U} \cdot 4\text{H}_2\text{O}$ (1), $\text{Co}(\text{NO}_3)_2 \cdot 6\text{U}$ (3), $\text{FeCl}_2 \cdot 6\text{U} \cdot 3\text{H}_2\text{O}$ (5), and $\text{MnCl}_2 \cdot 3\text{U} \cdot 3\text{H}_2\text{O}$ complexes

REFERENCES

- [1] Wöhler, *Ann. Physik*, 12 (1828) 253.
- [2] Jr. Tonn, *Chem. Eng.*, 62 (1955) 186.
- [3] P. Moore, *Chem. & Eng. News*, 37 (1959) 84.
- [4] A. Franz, *J. Org. Chem.*, 26 (1961) 3304.
- [5] D. Feldman, A. Barbalata, "Synthetic Polymers", Chapman & Hall, London (1996).
- [6] I. L. Finar, "Organic Chemistry", Longman group limited, London (1973) P. 460.
- [7] M. J. Rahman, P. Bozadjiev and Y. Polovski, *fert. Res.*, 38(2) (1994) 89.
- [8] S. George, M. Chellapandian, B. Sivasankar, K. Jayaraman, *Bioprocess Eng.*, 16(2) (1997) 83.
- [9] X. J. Wang, L.A. Douglas, *Agrochimica*, 40(5-6) (1996) 209.
- [10] O. A. Yerokun, *S. Afr. J. plant soil*, 14(2) (1997) 63.
- [11] R. Heinig, *SOFW J.*, 122(14) (1996) 998.
- [12] C. T. Gnewuch, G. Sosnovsky, *Chem. Rev.*, 97(3) (1997) 829.
- [13] C. I. Miyagawa, *Drug Intell. & Clin. Pharma.*, 20 (1986) 527.
- [14] E. Kissa, *Text. Res. J.*, 39(8) (1969) 734.
- [15] I. Srinivasa, K. Vishivanathapuram, M. B. Mishra, S. K. Ghosh, *Technology*, 7(12) (1970) 27.
- [16] I. M. Kaganskii, A. M. Babenko, *Zh. Prikl. Khim.*, 43(11) (1970) 2390.
- [17] Y. Zhang, J. Bai, T. Wei, A. Lu, *Huaxue Shijie*, 37(4) (1996) 178.
- [18] Y.K. Kim, J.W. Williard, A.W. Frazier, *J. Chem. Eng. Data*, 33(3) (1988) 306.
- [19] Hu. Chuncong, *Chem. Abs.*, 113, 888 (1990).
- [20] A.D. Pandey, L. Singh, R. Yadav, K. M. Varma, *Chem. Abs.*, 118 (1993) 607.
- [21] A. Crispoldi, *Chem. Abs.*, 119 (1993) 831.
- [22] M. Sugimura, Y. Kameyama, T. Hashimoto, T. Kobayashi, S. Muramatsu. *Chem. Abs.*, 112 (1990) 63.
- [23] P. S. Gentile, P. Carfagno, S. Haddad, L. Campisi, *Inorg. Chim. Acta*, 6(C) (1972) 296.
- [24] D. S. Sagatys, R. C. Bott, G. Smith, K. A. Byriel, C. H. L. Kennard, *Polyhedron*, 11(1) (1992) 49.
- [25] K. Lewinski, J. Sliwinski, L. Lebioda, *Inorg. Chem.*, 22(16) (1983) 2339.
- [26] S. V. Kryatov, A. Y. Nazarenko, P. D. Robinson, E. V. Rybak-Akimova, *Chemical Communications*, 11 (2000) 921.
- [27] T. J. Bhoopathy, M. Baskaran, S. Mohan, *Indian J. Phys.*, 62 B (1) (1988) 47.
- [28] A. Yamaguchi, R. B. Penland, S. Mizushima, T. J. Lane, Columba Curran, J. V. Quagliano, *J. Amer. Chem. Soc.*, 80 (1958) 527.
- [29] J. L. Duncan, *Spectrochim. Acta, Part A*, 27 (1970) 1197.
- [30] G. B. Aitken, J. L. Duncan, G. P. Mc Quillan, *J. Chem. Soc. A*, 2695, (1971).
- [31] D. Hadzi, J. Kidric, Z. V. Knezevic, B. Barlic, *Spectrochim. Acta, Part A*, 32 (1976) 693.
- [32] Sib Sankar Bala, Pradip N. Ghosh, *J. Mol. Str.*, 101 (1983) 69.
- [33] L. Kellner, *Proc. Roy. Soc.*, A 177 (1941) 456.
- [34] R. D. Waldron, R. M. Badger, *J. Chem. Phys.*, 18 (1950) 566.

- [35] E. R. Andrew, D. Hyndman, *Proc. Phys. Soc.*, A 66 (1953) 1187.
- [36] A. Yamaguchi, T. Miyazawa, T. Shimanouchi, S. Mizushima, *Spectrochim. Acta*, 10 (1957) 170.
- [37] J. E. Stewart, *J. Chem. Phys.*, 26 (1957) 248.
- [38] R. B. Penland, S. Mizushima, C. Curran, J. V. Quagliano, *J. Amer. Chem. Soc.*, 79 (1957) 1575.
- [39] G. F. Svatos, C. Curran, J. V. Quagliano, *This Journal*, 77 (1965) 6159.
- [40] W. F. Boron and E. L. Boulpaep, *Medical Physiology*, Updated Edition, Saunders, Philadelphia, Pa, USA, 2004.
- [41] J. H. Meessen and H. Petersen, "Urea," in Ullmann's Encyclopedia of Industrial Chemistry, Electronic Release, Wiley-VCH, Weinheim, Germany, 6th edition, 2002.
- [42] A.W. Bauer, W.M. Kirby, C. Sherris, M. Turck, *Amer. J. Clinical Pathology*, 45 (1966) 493.
- [43] M.A. Pfaller, L. Burmeister, M.A. Bartlett, M.G. Rinaldi, *J. Clin. Microbiol.* 26 (1988) 1437.
- [44] National Committee for Clinical Laboratory Standards, Performance Vol. antimicrobial susceptibility of Flavobacteria, 1997.
- [45] National Committee for Clinical Laboratory Standards. 1993. Methods for dilution antimicrobial susceptibility tests for bacteria that grow aerobically. Approved standard M7-A3. National Committee for Clinical Laboratory Standards, Villanova, Pa.
- [46] National Committee for Clinical Laboratory Standards. (2002). Reference Method for Broth Dilution Antifungal Susceptibility Testing of Conidium-Forming Filamentous Fungi: Proposed Standard M38-A. NCCLS, Wayne, PA, USA.
- [47] National Committee for Clinical Laboratory Standards. (2003). Methods for Antifungal Disk Diffusion Susceptibility Testing of Yeast: Proposed Guideline M44-P. NCCLS, Wayne, PA, USA.
- [48] L.D. Liebowitz, H.R. Ashbee, E.G.V. Evans, Y. Chong, N. Mallatova, M. Zaidi, D. Gibbs, and Global Antifungal Surveillance Group. 2001. *Diagn. Microbiol. Infect. Dis.* 4, 27.
- [49] M.J. Matar, L. Ostrosky-Zeichner, V.L. Paetznick, J.R. Rodriguez, E. Chen, J.H. Rex, 2003. *Antimicrob. Agents Chemother.*, 47, 1647.
- [50] A. Earnshaw, "Introduction to Magnetochemistry" Academic press, London and New York, pp. 35, 1968.
- [51] R. Keuleers, H.O. Desseyn, B. Rousseau, C. Van Alsenoy, *J. Phys. Chem. A*, 103(24) (1999) 4621.
- [52] E. Diamantopoulou, G.S. Papaefstathiou, A. Terzis, C.P. Raptopoulou, H.O. Desseyn, S. P. Perlepes, *Polyhedron*, 22 (2003) 825.
- [53] R. Keuleers, G.S. Papaefstathiou, C.P. Raptopoulou, S.P. Perlepes, H.O. Desseyn, *J. Mol. Str.*, 525(1-3) (2000) 173.
- [54] K. Nakamoto "Infrared and Raman Spectra of Inorganic and Coordination Compounds", Wiley, New York, 1978.
- [55] C.X. Quan, L.H. Bin, G.G. Bang, *Mater. Chem. Phys.* 91 (2005) 317.